EURASIP Journal on Wireless Communications and Networking

RESEARCH Open Access

Dual-polarized IRS-assisted wireless network: relative phase modulation

Muteen Munawar[1] and Kyungchun Lee[1*]

*Correspondence:
kclee@seoultech.ac.kr

[1] Department of Electrical and Information Engineering and the Research Center for Electrical and Information Technology, Seoul National University of Science and Technology, Nowon-gu, 01811 Seoul, Republic of Korea

Abstract

The metasurface is a promising technology that can help next-generation wireless communication systems not only improve the signal-to-noise ratio (SNR), but also increase security and mitigate interference. Further, introducing dual polarization (DP) in a metasurface can enhance its capabilities with polarization diversity, polarization multiplexing, and polarization-switched modulation. In this paper, we study a DP-metasurface-assisted single-user wireless communication system and propose a novel scheme that can improve the spectral efficiency (SE) and bit-error-rate (BER) performance compared to those of conventional schemes by exploiting the orthogonal property of dual-polarized waves. We employ the DP metasurface to increase the SNR at the receiver and create a specific phase difference between the polarized signals by controlling the transmit precoder and the phases of the metasurface reflecting elements representing some modulated bits. At the receiver, we use the recovered phase information to realign the modulated symbols in both polarizations, which are then added coherently. The simulation results demonstrate that the proposed scheme achieves significantly higher SE and BER performance than those of some closely related works.

Keywords: Intelligent reflecting surface, Metasurface, Dual polarization, Relative phase modulation, SNR maximization

1 Introduction

A reflecting surface containing multiple reflecting elements with different phases is not a new concept in the literature [1]. However, recent progress in metamaterials, through which the phases and amplitudes of reflected signals can be controlled in real time by changing the material properties via biasing voltages [2, 3], has demonstrated their potential applications in next-generation wireless communication systems [4]. In the literature, such metasurfaces are called intelligent reflecting surface (IRS) [4], reconfigurable intelligent surface (RIS) [5–7], smart reflect arrays [8–10], and many other names [11–14]. In this paper, we use the term IRS. There are many publications regarding low-complexity schemes to optimize IRS operations to maximize the signal-to-noise ratio (SNR) [13, 15–21], as well as channel-estimation methods for IRS-assisted communication systems [13, 21, 22]. Specifically, in [15] and [16], the authors used alternating optimization (AO) and adaptive-selection beamforming, respectively, to maximize the

received SNR by optimizing the transmit precoding vector and IRS passive phases for ideal IRSs. In [17], the authors extended the AO algorithm to a practical IRS, that is, discrete phases. Similarly, in [18] and [19], the authors presented beamforming methods for IRS-assisted multiple-input single-output (MISO) and multiple-input multiple-output (MIMO) wireless networks.

Dual polarization (DP) is a potential way to improve the performance of communication systems. For example, it can provide polarization diversity (PD) gains [23], polarization multiplexing (PM) gains [24], and an extra dimension to modulate the data, i.e., PS-QPSK [25]. Similarly, DP in IRS elements can further enhance the capabilities of IRS. In [26], the authors used dual-polarized IRS (DP-IRS) multiplexing and divided the users into two groups, one assigned to horizontal polarization and the other to vertical polarization, to compete with interfering users. In [27], the authors proposed modulating the data directly on the reflecting elements in the DP-IRS. They used a simple radio-frequency (RF) source to generate a constant signal and controlled the DP-IRS elements such that the reflected signals from all elements were coherently combined at the user to construct a modulation symbol. Although the scheme in [27] helped reduce the RF chains, the performance was lower than that of the simple (single-polarized) IRS because there is only one communication path, whereas the simple IRS employs two paths for communication, i.e., the direct and reflected paths. To the best of our knowledge, few studies have researched the use of DP-IRS.[1] However, we believe that it has far more potential than simple IRS in terms of PD and PM gains, and an extra dimension for modulation.

1.1 Methods/experimental

In this paper, we consider a wireless communication network with a DP-IRS-assisted single-antenna user, where the access point (AP) and user are equipped with dual-polarized antennas. Each antenna is connected to one RF chain but separate phase shifters for polarizations, whose vertical and horizontal radiation patches are closely spaced leading to no PD gain [28]. For the DP-IRS network, we propose a novel scheme that enhances the SNR while simultaneously modulating some data in the orthogonal dimension of DP-IRS, which helps to improve the bit-error-rate (BER) and spectral efficiency (SE) as compared to a simple IRS. Specifically, we control the transmit digital filter, transmit passive filters, DP-IRS operations, and receive passive filters such that one of the polarized signals (say horizontal) reaches the user with a different phase as compared to the other polarized signal (say vertical). This relative phase shift is determined by the information bits at the AP. We estimate the phase shift at the user and rotate back the horizontal symbol to align it with the vertical symbol to provide higher combined signal power for demodulation. We also use the recovered phase shift to demodulate some information bits; finally, we combine both demodulated bits to obtain the entire transmitted data. It is noted that applying this scheme makes the performance of these two modulations mutually dependent. For example, if the recovered phase shift is in error, then the final recovered symbol may also be in error because that erroneous phase shift

[1] Elaboration on DP-IRS is available in [26, 28, 31], and for brevity, these details are not reiterated here.

leads to inaccurate combining of polarized signals. However, the proper selection of modulation levels for the proposed scheme can result in better performance than that of the simple IRS.

1.2 Contributions

Our main contributions are as follows:

- We study a DP-IRS-assisted wireless network and propose a novel scheme that not only exploits DP-IRS for signal strength enhancement but also introduces a novel relative phase modulation.
- To solve the formulated non-convex optimization problem, we first derive closed-form optimal solutions for DP-IRS operations, transmit digital filter, and transmit/receive DP antenna phase shifters. Finally, based on the derived solutions, we propose a novel multistep AO algorithm.
- Lastly, we provide an extensive numerical analysis of the proposed scheme and compare it with relevant benchmark schemes.

The remainder of the paper is organized as follows: Section II introduces the mathematical model of our proposed system, and Section III discusses the problem formulation. In Section IV, we describe the proposed scheme and solve a power-maximization problem related to our system model. Section V presents a numerical evaluation of the proposed scheme and a comparison with some closely related works. Finally, Section VI concludes the paper.

1.3 Notations

Scalars are denoted by italic letters, whereas vectors and matrices are denoted by boldface lower-case and upper-case letters, respectively. For a complex-valued vector $\mathbf{v}$, $(\mathbf{v})^T$ denotes the transpose, $(\mathbf{v})^H$ denotes the conjugate transpose, $|\mathbf{v}|$ denotes the element-wise absolute value, $\|\mathbf{v}\|$ denotes the Euclidean norm, diag($\mathbf{v}$) denotes a diagonal matrix with each diagonal element being the corresponding element in $\mathbf{v}$, and arg($\mathbf{v}$) denotes a vector with each element being the phase of the corresponding element in $\mathbf{v}$. For a complex-valued square matrix $\mathbf{A}$, $\mathbf{I_A}$ denotes an identity matrix of size $\mathbf{A}$, $\mathbf{A}^\dagger$ denotes the pseudoinverse, $\|\mathbf{A}\|$ denotes the Frobenius norm, det ($\mathbf{M}$) denotes the determinant, and $\mathbf{A} \circ \mathbf{A}$ denotes the Hadamard product. The notation $(\cdot)^*$ indicates the complex conjugate of a complex number.

2 System model

The system model considered in this paper is shown in Fig. 1, where a DP-IRS assists MISO communication between an AP and a single DP antenna user. We assume narrowband frequency-flat channels for all links. The AP has N_t DP antennas, each of which is equipped with a single RF chain but separate phase shifters for polarizations [29, 30], as shown in Fig. 2. The DP-IRS has N elements and the operation of each element can be defined by the following transformation matrix [26]:

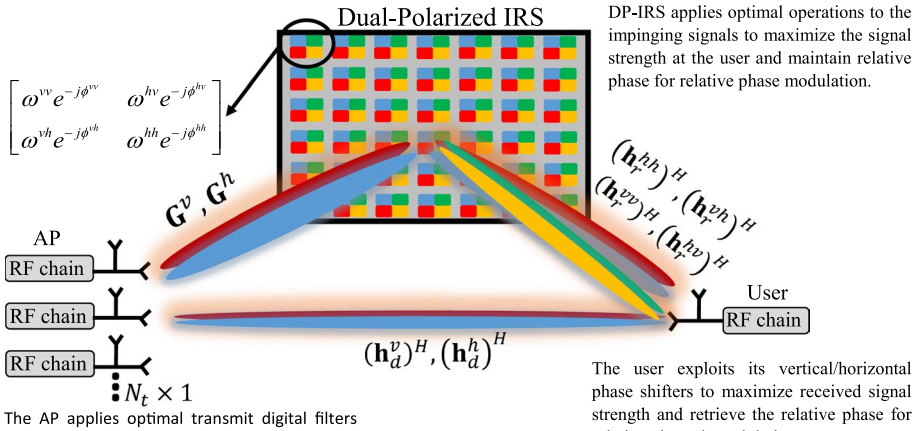

Fig. 1 System model

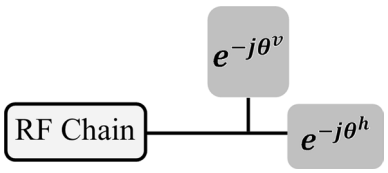

Fig. 2 Dual-polarized antenna with separate phase shifters

$$\boldsymbol{\Psi} = \begin{bmatrix} \omega^{vv} e^{-j\phi^{vv}} & \omega^{hv} e^{-j\phi^{hv}} \\ \omega^{vh} e^{-j\phi^{vh}} & \omega^{hh} e^{-j\phi^{hh}} \end{bmatrix}, \tag{1}$$

where ω^{pq} and ϕ^{pq} indicate the reflected signal's amplitude and phase changes from polarization p to q, respectively, and $p, q \in \{v, h\}$, whereas v and h indicate vertical and horizontal polarization, respectively. Each subpart of the reflecting element provides independent control, i.e., reflection and conversion, over each polarization [26, 32–34]. The signal received at the user is the combination of two signals coming from the AP and DP-IRS. We start with a signal model, where the AP and DP-IRS have only one antenna and one reflecting element, respectively. Then, the total noiseless signal received at the user is given by

$$\begin{aligned} \begin{bmatrix} y^v \\ y^h \end{bmatrix} = & \begin{pmatrix} e^{-j\gamma^v} & 0 \\ 0 & e^{-j\gamma^h} \end{pmatrix} \Bigg[\Bigg\{ \begin{pmatrix} (h_r^{vv})^* & (h_r^{hv})^* \\ (h_r^{vh})^* & (h_r^{hh})^* \end{pmatrix} \\ & \circ \underbrace{\begin{pmatrix} \omega^{vv} e^{-j\phi^{vv}} & \omega^{hv} e^{-j\phi^{hv}} \\ \omega^{vh} e^{-j\phi^{vh}} & \omega^{hh} e^{-j\phi^{hh}} \end{pmatrix}}_{\boldsymbol{\Psi}} \circ \begin{pmatrix} g^{vv} & g^{hv} \\ g^{vh} & g^{hh} \end{pmatrix} \\ & + \begin{pmatrix} (h_d^v)^* & 0 \\ 0 & (h_d^h)^* \end{pmatrix} \Bigg\}^T \begin{pmatrix} \sqrt{\frac{P_t}{2}} e^{-j\theta^v} & 0 \\ 0 & \sqrt{\frac{P_t}{2}} e^{-j\theta^h} \end{pmatrix} \Bigg]^T \mathbf{w}x, \end{aligned} \tag{2}$$

where y^v and y^h are the horizontal and vertical polarized signals received at the user. Furthermore, $(h_r)^*$, $(h_d)^*$, and g denote the channels of IRS-user link, AP-user link, and AP-IRS link, respectively, whereas $\mathbf{w}$ and x are the transmit digital filter and transmitted symbol, respectively. The matrices $\text{diag}\left(\sqrt{\frac{P_t}{2}}e^{-j\theta^v}, \sqrt{\frac{P_t}{2}}e^{-j\theta^h}\right)$ and $\text{diag}\left(e^{-j\gamma^v}, e^{-j\gamma^h}\right)$ in (2) represent the passive phase shifters at the AP and user, respectively. In (2), the total transmission power P_t is divided equally between the two radiated polarizations because of a single RF chain. The combined noisy signal at the user can be written as

$$\begin{aligned} y =& y^v + y^h \\ =& \left(e^{-j\gamma^v}\left\{\left(h_r^{vv}\right)^*\omega^{vv}e^{-j\phi^{vv}}g^{vv} + \left(h_r^{hv}\right)^*\omega^{hv}e^{-j\phi^{hv}}g^{hv}\right.\right. \\ &\left.\left. + \left(h_d^v\right)^*\right\}\sqrt{\frac{P_t}{2}}e^{-j\theta^v}wx\right) + \left(e^{-j\gamma^h}\left\{\left(h_r^{vh}\right)^*\omega^{vh}e^{-j\phi^{vh}}g^{vh}\right.\right. \\ &\left.\left. + \left(h_r^{hh}\right)^*\omega^{hh}e^{-j\phi^{hh}}g^{hh} + \left(h_d^h\right)^*\right\}\sqrt{\frac{P_t}{2}}e^{-j\theta^h}wx\right) + z, \end{aligned} \tag{3}$$

where z is additive white Gaussian noise with zero mean and σ^2 variance.

We note that there is no PD[2] in this system because both polarized signals are radiated by a single DP antenna, reflected by a single DP-IRS element, and then received by a single DP antenna, going through the same channels [28], i.e., $h_r^{pp} = h_r^{pq} = h_r$, $h_d^p = h_d^q = h_d$, and $g^{pp} = g^{pq} = g$. Hence, we can set $e^{-j\phi^{vv}} = e^{-j\phi^{hv}} = e^{-j\phi^v}$ and $e^{-j\phi^{vh}} = e^{-j\phi^{hh}} = e^{-j\phi^h}$. Furthermore, for the proposed work, we assume full reflection from all elements, which can be achieved by setting $\omega^{vv} = \omega^{hv} = \omega^{vh} = \omega^{hh} = 1$. More details on the dual-polarized channel models are provided in [26, 28, 31] and hence omitted here for brevity. The signal model in (3) can be simplified as

$$\begin{aligned} y =& \left(\left(e^{-j\gamma^v}\left\{h_r^*e^{-j\phi^v}g + h_d^*\right\}e^{-j\theta^v}\right)\right. \\ &\left. + \left(e^{-j\gamma^h}\left\{h_r^*e^{-j\phi^h}g + h_d^*\right\}e^{-j\theta^h}\right)\right)\sqrt{\frac{P_t}{2}}wx + z.s \end{aligned} \tag{4}$$

The signal model (4) can be extended for N_t transmit antennas and N reflecting elements in the following form:

$$\begin{aligned} y =& \left(\left(e^{-j\gamma^v}\left\{\mathbf{h}_r^H\mathbf{\Phi}^v\mathbf{G} + \mathbf{h}_d^H\right\}\mathbf{U}^v\right)\right. \\ &\left. + \left(e^{-j\gamma^h}\left\{\mathbf{h}_r^H\mathbf{\Phi}^h\mathbf{G} + \mathbf{h}_d^H\right\}\mathbf{U}^h\right)\right)\mathbf{w}x + z, \end{aligned} \tag{5}$$

where $\mathbf{G}$, $\mathbf{h}_r^H$, and $\mathbf{h}_d^H$ are baseband equivalent channels having the sizes of $N \times N_t$, $1 \times N$, and $1 \times N_t$, respectively, with complex-valued entries, whereas $\mathbf{w}$ is $N_t \times 1$ transmit digital filter, and $\mathbf{\Phi}^v$ and $\mathbf{\Phi}^h$ are $N \times N$ diagonal matrices containing the phase controls of the DP-IRS elements in diagonal, e.g., $\mathbf{\Phi}^v = \text{diag}(e^{-j\phi_1^v}, e^{-j\phi_2^v}, \ldots, e^{-j\phi_N^v})$. In

[2] To avoid the intricate mathematical formulations, we posit the absence of polarization diversity gains in the system. Nonetheless, it is noteworthy that the proposed algorithm and problem formulation exhibit applicability to scenarios involving generic channel models.

addition, the matrices $\mathbf{U}^v \in \mathbb{C}^{N_t \times N_t}$, and $\mathbf{U}^h \in \mathbb{C}^{N_t \times N_t}$ contain the transmit vertical, transmit horizontal phase shifters in the diagonal, respectively, i.e., $\mathbf{U}^p = \text{diag}\left(e^{-j\theta_1^p}, e^{-j\theta_2^p}, e^{-j\theta_3^p}, \ldots, e^{-j\theta_{N_t}^p}\right)$, where $p \in \{v, h\}$. The received signal strength can be written as

$$s = \left| \left(e^{-j\gamma^v} \left\{\mathbf{h}_r^H \mathbf{\Phi}^v \mathbf{G} + \mathbf{h}_d^H\right\} \mathbf{U}^v\right) + \left(e^{-j\gamma^h} \left\{\mathbf{h}_r^H \mathbf{\Phi}^h \mathbf{G} + \mathbf{h}_d^H\right\} \mathbf{U}^h\right) \mathbf{w} \right|^2, \tag{6}$$

which can be maximized by optimizing $\mathbf{w}$, $\mathbf{\Phi}^p$, $\mathbf{U}^p$, and γ^p, where $p \in \{v, h\}$.

To exploit the DP for signal modulation, polarization-switched (PS) modulation [25] can be considered, where data are transmitted in v/h polarization at a time determined by input bits 0/1, thus creating an extra dimension to modulate one bit of data. However, PS modulation with DP-IRS is not very beneficial, as it makes inefficient use of the DP-IRS by toggling its v and h polarization reflections to modulate each bit of data.

In the next section, we propose a dual-polarized IRS-assisted scheme, which can improve the SE and BER simultaneously. Specifically, we control the transmit digital filter $\mathbf{w}$, transmit passive filters ($\mathbf{U}^v$ and $\mathbf{U}^h$), DP-IRS operations ($\mathbf{\Phi}^v$ and $\mathbf{\Phi}^h$), and receive passive filters (γ^v and γ^h) in (5) to not only enhance the signal power (6), but also to create a specific phase difference λ between two polarized received signals, i.e., $e^{-j\gamma^v}\left(\mathbf{h}_r^H \mathbf{\Phi}^v \mathbf{G} + \mathbf{h}_d^H\right)\mathbf{U}^v \mathbf{w} = y^v$ and $e^{-j\gamma^h}\left(\mathbf{h}_r^H \mathbf{\Phi}^h \mathbf{G} + \mathbf{h}_d^H\right)\mathbf{U}^h \mathbf{w} = y^h$. Here, λ is determined by the input data bits at the AP.

3 Problem formulation: SNR maximization and modulation

As mentioned previously, we need to control $\mathbf{w}$, ($\mathbf{U}^v$,$\mathbf{U}^h$), and $\left(\mathbf{\Phi}^v, \mathbf{\Phi}^h\right)$ in (6) to maximize the signal power $|y|^2$ and create a phase difference λ between y^v and y^h. Specifically, we set one of the polarization signal to a reference (say y^v) and ensure that it is received with zero phase rotation, i.e., $y^v = \beta^v e^{j0} x$ under a no-noise assumption, where $\beta^v = \left|\left(\mathbf{h}_r^H \mathbf{\Phi}^v \mathbf{G} + \mathbf{h}_d^H\right)\mathbf{U}^v \mathbf{w}\right|$ and $\arg\left(\left(\mathbf{h}_r^H \mathbf{\Phi}^v \mathbf{G} + \mathbf{h}_d^H\right)\mathbf{U}^v \mathbf{w}\right) = 0$. Similarly, we ensure that the signal received with horizontal polarization has a phase difference with respect to the vertical signal, i.e., $y^h = \beta^h e^{j\lambda} x$ under a no-noise assumption, where $\beta^h = \left|\left(\mathbf{h}_r^H \mathbf{\Phi}^h \mathbf{G} + \mathbf{h}_d^H\right)\mathbf{U}^h \mathbf{w}\right|$ and $\arg\left(\left(\mathbf{h}_r^H \mathbf{\Phi}^h \mathbf{G} + \mathbf{h}_d^H\right)\mathbf{U}^h \mathbf{w}\right) = \lambda$. For power-maximization and relative phase (RP) modulation, the problem can be formulated as follows:

$$\begin{aligned}
&\max_{\mathbf{w}, \mathbf{U}^v, \mathbf{U}^h, \Phi^v, \Phi^h, \gamma^v, \gamma^h} |((e^{-j\gamma^v}\{\mathbf{h}_r^H \Phi^v \mathbf{G} + \mathbf{h}_d^H\})\mathbf{U}^v) + (e^{-j\gamma^h}\{\mathbf{h}_r^H \Phi^h \mathbf{G} + \mathbf{h}_d^H\})\mathbf{U}^h)\mathbf{w}| \\
&\text{s.t.} \quad \|\mathbf{w}\|^2 \le \frac{P_t}{2}, \quad \mathbf{U}^p = \text{diag}\left(e^{-j\theta_1^p}, e^{-j\theta_2^p}, \ldots, e^{-j\theta_{N_t}^p}\right), p \in \{v, h\}, \\
&\quad \Phi^p = \text{diag}\left(e^{-j\phi_1^p}, e^{-j\phi_2^p}, \ldots, e^{-j\phi_N^p}\right), p \in \{v, h\}, \\
&\quad \arg\left(\left(\mathbf{h}_r^H \Phi^v \mathbf{G} + \mathbf{h}_d^H\right)\mathbf{U}^v \mathbf{w}\right) = 0, \quad \arg\left(\left(\mathbf{h}_r^H \Phi^h \mathbf{G} + \mathbf{h}_d^H\right)\mathbf{U}^h \mathbf{w}\right) = \lambda.
\end{aligned} \tag{P1}$$

The first constraint in problem (P1), i.e., $\|\mathbf{w}\|^2 \le \frac{P_t}{2}$, is due to a single RF chain per DP-antenna, and ϕ_n^p and $\theta_{n_t}^p$ indicate the nth and n_tth diagonal entries of $\mathbf{\Phi}^p$ and $\mathbf{U}^p$, respectively, where $p \in \{v, h\}$. The last two constraints, i.e., $\arg\left(\left(\mathbf{h}_r^H \mathbf{\Phi}^v \mathbf{G} + \mathbf{h}_d^H\right)\mathbf{U}^v \mathbf{w}\right) = 0$ and $\arg\left(\left(\mathbf{h}_r^H \mathbf{\Phi}^h \mathbf{G} + \mathbf{h}_d^H\right)\mathbf{U}^h \mathbf{w}\right) = \lambda$, denote the pro-

posed RP modulation. The objective function of (P1) can be demonstrated to be a non-convex over $\mathbf{w}$, $\mathbf{U}_v$, $\mathbf{U}_h$, $\mathbf{\Phi}_v$, and $\mathbf{\Phi}_h$. In the following section, we propose a multi-step AO algorithm to efficiently solve this problem.

4 Proposed solution to problem (P1)

Here, we describe the framework of the proposed algorithm. Specifically, we first divide the problem (P1) into several non-convex subproblems, which are solved separately. Then, we propose the AO algorithm, which solves the subproblems alternately until the objective function converges.

4.1 Optimal transmit digital filter

Here, we reformulate the problem (P1) to find the optimal transmit digital filter. For the formulation, we assume $\mathbf{U}^v = \mathbf{U}^h = \mathbf{\Phi}^v = \mathbf{\Phi}^h = \mathbf{I}$ and $\gamma^v = \gamma^h = 0$. Correspondingly, the problem (P1) is written as

$$\begin{aligned} &\max_{\mathbf{w}} \ \left|\mathbf{h}^H\mathbf{w}\right| \\ &\text{s.t.} \quad \|\mathbf{w}\|^2 \le \frac{P_t}{2}, \\ &\quad \mathbf{h}^H = \left(\left(e^{-j\gamma^v}\left\{\mathbf{h}_r^H\mathbf{\Phi}^v\mathbf{G} + \mathbf{h}_d^H\right\}\mathbf{U}^v\right)\right. \\ &\quad \left. + \left(e^{-j\gamma^h}\left\{\mathbf{h}_r^H\mathbf{\Phi}^h\mathbf{G} + \mathbf{h}_d^H\right\}\mathbf{U}^h\right)\right), \end{aligned} \tag{P1.1}$$

which is a conventional precoder designing problem for single-user MISO system. Hence, the optimal $\mathbf{w}$ is given by the maximum-ratio transmission:

$$\mathbf{w} = \sqrt{\frac{P_t}{2}} \frac{\left(\left(e^{-j\gamma^v}\left\{\mathbf{h}_r^H\mathbf{\Phi}^v\mathbf{G} + \mathbf{h}_d^H\right\}\mathbf{U}^v\right) + \left(e^{-j\gamma^h}\left\{\mathbf{h}_r^H\mathbf{\Phi}^h\mathbf{G} + \mathbf{h}_d^H\right\}\mathbf{U}^h\right)\right)^H}{\left\|\left(e^{-j\gamma^v}\left\{\mathbf{h}_r^H\mathbf{\Phi}^v\mathbf{G} + \mathbf{h}_d^H\right\}\mathbf{U}^v\right) + \left(e^{-j\gamma^h}\left\{\mathbf{h}_r^H\mathbf{\Phi}^h\mathbf{G} + \mathbf{h}_d^H\right\}\right)\mathbf{U}^h\right\|} e^{j\eta}, \tag{7}$$

where η is an extra phase shift to satisfy $\arg\left(\left(\mathbf{h}_r^H\mathbf{\Phi}^v\mathbf{G} + \mathbf{h}_d^H\right)\mathbf{U}^v\mathbf{w}\right) = 0$. Specifically, in each iteration of AO algorithm, we select η such that $\arg\left(\mathbf{h}_d^H\mathbf{U}^v\mathbf{w}\right) = 0$, leading to

$$\eta = -\arg\left(\mathbf{h}_d^H\mathbf{U}^v\mathbf{w}\right). \tag{8}$$

More details are provided in Algorithm 1.

4.2 DP-IRS phases optimization

Given $\mathbf{w}$ from (7), assuming $\mathbf{U}^v = \mathbf{U}^h = \mathbf{I}$, $\gamma^v = \gamma^h = 0$, and defining $e^{-j\gamma^p}\mathbf{h}_d^H\mathbf{U}^p\mathbf{w} = \beta^p$, $e^{-j\gamma^p}\mathbf{h}_r^H = \mathbf{h}_r'^H$, and $\mathbf{h}_r'^H\mathbf{\Phi}^p\mathbf{G}\mathbf{U}^p\mathbf{w} = \left(\mathbf{l}^p\right)^H\boldsymbol{\alpha}^p$ where

$\mathbf{v}^p = \left[e^{-j\phi_1^p}, e^{-j\phi_2^p}, \ldots, e^{-j\phi_N^p}\right]^H$, $\boldsymbol{\alpha}^p = \text{diag}\left(\mathbf{h}_r^{'H}\right)\mathbf{G}\mathbf{U}^p\mathbf{w}$, and $p \in \{v, h\}$, the problem (P1) for $\left(\boldsymbol{\Phi}^v, \boldsymbol{\Phi}^h\right)$ can be written as

$$\begin{aligned} &\max_{\mathbf{l}^v, \mathbf{l}^h} \left| \left(\mathbf{l}^v\right)^H \boldsymbol{\alpha}^v + \beta^v + \left(\mathbf{l}^h\right)^H \boldsymbol{\alpha}^h + \beta^h \right| \\ &\text{s.t.} \left|\mathbf{l}_{(n)}^p\right| = 1, \quad n = 1, 2, \ldots, N, \; p \in \{v, h\}. \end{aligned} \tag{P1.2}$$

Next we solve (P1.2) for $\left(\mathbf{l}^v, \mathbf{l}^h\right)$.

4.2.1 Optimization of $\mathbf{l}^v$

Assuming $\mathbf{l}^h = [1, 1, \ldots, 1]^T$ and defining $\beta^{'v} = \beta^v + \left(\mathbf{l}^h\right)^H \boldsymbol{\alpha}^h + \beta^h$ the problem (P1.2) for $\mathbf{l}^v$ can be written as

$$\begin{aligned} &\max_{\mathbf{l}^v} \left| \left(\mathbf{l}^v\right)^H \boldsymbol{\alpha}^v + \beta^{'v} \right| \\ &\text{s.t.} \quad \left|\mathbf{l}_{(n)}^v\right| = 1, \; n = 1, 2, \ldots, N. \end{aligned} \tag{P1.3}$$

To address (P1.3), it is necessary to ensure that $\arg\left(\left(\mathbf{l}^v\right)^H \boldsymbol{\alpha}^v\right) = \arg\left(\beta^{'v}\right)$. Let $\arg\left(\beta^{'v}\right) = \gamma^v$, (P1.3) can be reformulated as

$$\begin{aligned} &\max_{\mathbf{l}^v} \left| \left(\mathbf{l}^v\right)^H \alpha^v \right| \\ &\text{s.t.} \quad \left|\mathbf{l}_{(n)}^v\right| = 1, \; n = 1, 2, \ldots, N, \\ &\quad \arg\left(\beta^{'v}\right) = \gamma^v. \end{aligned} \tag{P1.4}$$

The optimal solution for (P1.4) can be readily derived as $\mathbf{l}^{v*} = e^{j\left(\arg\left(\beta^{'v}\right) - \arg\left(\boldsymbol{\alpha}^v\right)\right)}$, and correspondingly, the nth phase shift for the vertical part of the DP-IRS is given by

$$\phi_{(n)}^v = \arg\left(\beta^{'v}\right) - \arg\left(\boldsymbol{\alpha}_{(n)}^v\right), \; n = 1, 2, \ldots, N. \tag{9}$$

4.2.2 Optimization of $\mathbf{l}^h$

Given $\mathbf{l}^v$ from (9) and defining $\beta^{'h} = \beta^h + \left(\mathbf{l}^v\right)^H \boldsymbol{\alpha}^v + \beta^v$ the problem (P1.2) for $\mathbf{l}^h$ can be written as

$$\begin{aligned} &\max_{\mathbf{l}^h} \left| \left(\mathbf{l}^h\right)^H \boldsymbol{\alpha}^h + \beta^{'h} \right| \\ &\text{s.t.} \quad \left|\mathbf{l}_{(n)}^h\right| = 1, \; n = 1, 2, \ldots, N. \end{aligned} \tag{P1.5}$$

Utilizing a procedure similar to that employed for $\mathbf{l}^v$ in (P1.3), one can deduce the optimal solution for (P1.5) as $\mathbf{l}^{h*} = e^{j\left(\arg\left(\beta^{'h}\right) - \arg\left(\boldsymbol{\alpha}^h\right)\right)}$, leading to the following nth optimal phase shift for the horizontal part of DP-IRS:

$$\phi_{(n)}^h = \arg\left(\beta^{'h}\right) - \arg\left(\boldsymbol{\alpha}_{(n)}^h\right), \; n = 1, 2, \ldots, N. \tag{10}$$

4.3 Optimal phase shifters for transmit DP antennas

Given $\mathbf{w}$, $\mathbf{\Phi}^v$, and $\mathbf{\Phi}^h$ from (7), (9), and (10), respectively, assuming $\gamma^v = \gamma^h = 0$, and defining $e^{-j\gamma^p}\left(\mathbf{h}_r^H \mathbf{\Phi}^p \mathbf{G} + \mathbf{h}_d^H\right)\mathbf{U}^p \mathbf{w} = \boldsymbol{\delta}^{p^H}\mathbf{u}^p$, where $\boldsymbol{\delta}^{p^H} = e^{-j\gamma^p}\left(\mathbf{h}_r^H \mathbf{\Phi}^p \mathbf{G} + \mathbf{h}_d^H\right)\text{diag}(\mathbf{w})$, $\mathbf{u}^p = \left[e^{-j\theta_1^p}, e^{-j\theta_2^p}, \ldots, e^{-j\theta_{N_t}^p}\right]$, and $p \in \{v, h\}$, the problem (P1) for $\left(\mathbf{U}^v, \mathbf{U}^h\right)$ can be written as

$$\begin{aligned} &\max_{\mathbf{u}^v, \mathbf{u}^h} \left|\boldsymbol{\delta}^{v^H}\mathbf{u}^v + \boldsymbol{\delta}^{h^H}\mathbf{u}^h\right| \\ &\text{s.t.} \quad \left|\mathbf{u}_{(n_t)}^h\right| = \left|\mathbf{u}_{(n_t)}^v\right| = 1,\ n_t = 1, 2, \ldots, N_t, \\ &\quad \arg\left(\left(\mathbf{h}_r^H \Phi^v \mathbf{G} + \mathbf{h}_d^H\right)\mathbf{U}^v \mathbf{w}\right) = 0, \quad \arg\left(\left(\mathbf{h}_r^H \Phi^h \mathbf{G} + \mathbf{h}_d^H\right)\mathbf{U}^h \mathbf{w}\right) = \lambda. \end{aligned} \tag{P1.6}$$

To solve (P1.6), one of the transmit phase shifters can be fixed and the other one can be optimized. Let $\mathbf{U}^v = \mathbf{I}$, and $\boldsymbol{\delta}^{v^H}\mathbf{u}^v = \rho^v$, then the problem (P1.6) for $\mathbf{u}^h$ can be written as

$$\begin{aligned} &\max_{\mathbf{u}^h} \left|\boldsymbol{\delta}^{h^H}\mathbf{u}^h + \rho^v\right| \\ &\text{s.t.} \quad \left|\mathbf{u}_{(n_t)}^h\right| = 1,\ n_t = 1, 2, \ldots, N_t \\ &\arg\left(\left(\mathbf{h}_r^H \Phi^h \mathbf{G} + \mathbf{h}_d^H\right)\mathbf{U}^h \mathbf{w}\right) = \lambda. \end{aligned} \tag{P1.7}$$

It can be easily shown that the optimal solution for (P1.7) is $\mathbf{u}^{h*} = e^{j\left(\arg\left(\rho^v\right) - \arg\left(\boldsymbol{\delta}^h\right)\right)}$, resulting in the following optimal phase shift for the n_tth element:

$$\theta_{(n_t)}^h = \arg\left(\rho^v\right) - \arg\left(\boldsymbol{\delta}_{(n_t)}^h\right),\ n_t = 1, 2, \ldots, N_t. \tag{11}$$

To satisfy the last constraint of (P1.7), we update $\mathbf{u}^h$ on symbol time as

$$\mathbf{u}^h = e^{j\lambda}\mathbf{U}^h \arg(\mathbf{w}). \tag{12}$$

In the following subsections, we explain how to determine and retrieve λ at the AP and receiver, respectively, while optimizing $\left(\gamma^v, \gamma^h\right)$.

4.4 DP-RP modulation

Considering that k bits are sent in one channel use, we choose m of k bits for M-QAM modulation, where $M = 2^m$. The remaining $l = k - m$ bits are chosen for L-RP modulation, where $L = 2^l$. To modulate l bits, we select 2^l equidistant phases from 0 to 2π:

$$\Omega = \left\{0,\ \frac{1}{2^l}2\pi,\ \frac{2}{2^l}2\pi,\ \frac{3}{2^l}2\pi,\ \ldots,\ \frac{(2^l - 1)}{2^l}2\pi\right\}. \tag{13}$$

For example, if $k = 10$ and $m = 8$, then we have $l = 2$. For $m = 8$ bits, we employ 256 -QAM modulation, and for $l = 2$ bits, we use four equidistant phases from 0 to 2π based on (13). Then, a 256-QAM symbol x is transmitted from both polarizations. However, the symbol sent over horizontal polarization has a relative phase difference λ with respect to the vertical polarization signal. This phase shift is selected from the set of equidistant phases, Ω.

4.5 RP recovery and demodulation

At the receiver, we estimate the relative phase difference λ and use it to align $\left(\mathbf{h}_r^H \mathbf{\Phi}^v \mathbf{G} + \mathbf{h}_d^H\right)\mathbf{U}^v\mathbf{w}$ with $\left(\mathbf{h}_r^H \mathbf{\Phi}^h \mathbf{G} + \mathbf{h}_d^H\right)\mathbf{U}^h\mathbf{w}$, i.e., y^v with y^h, which results in the combined signal $\hat{y}$ for QAM demodulation. Specifically, we set $\gamma^v = 0$ and determine $\hat{\lambda}$ by solving the following maximum-likelihood problem:

$$\hat{\lambda} = \arg \max_{\gamma^h \in \Omega} \left| e^{-j0} y^v + e^{-j\gamma^h} y^h \right|. \tag{P1.8}$$

After determining $\hat{\lambda}$, we exploit it to generate $\hat{y}$:

$$\hat{y} = y^v + e^{-j\hat{\lambda}} y^h. \tag{14}$$

Then, $\hat{y}$ is used for the QAM demodulation to recover m bits, whereas $\hat{\lambda}$ corresponds to the remaining l bits.

4.6 Overall algorithm

The presented AO algorithm sequentially tackles (P1.1), (P1.3), (P1.5), and (P1.7), continuing this process until convergence of the objective function for (P1). The assurance of convergence stems from the derivation of closed-form optimal solutions for each subproblem. A detailed description of the entire algorithm can be found in Algorithm 1.

Algorithm 1 Alternating Optimization Algorithm

1: Set iteration $i = 0$ and initialize $\mathbf{\Phi}_i^v = \mathbf{I}_{\mathbf{\Phi}^v}$, $\mathbf{\Phi}_i^h = \mathbf{I}_{\mathbf{\Phi}^h}$, $\mathbf{U}_i^v = \mathbf{I}_{\mathbf{U}^v}$, $\mathbf{U}_i^h = \mathbf{I}_{\mathbf{U}^h}$, and $\delta_{k,i}^v = \delta_{k,i}^h = \eta_i = 0$.
2: Given $\mathbf{U}_i^v$, $\mathbf{U}_i^h$, $\mathbf{\Phi}_i^v$, $\mathbf{\Phi}_i^h$, and η_i, calculate $\mathbf{w}_i$ and η_{i+1} using (7) and (8), respectively.
3: **repeat**
4: Given $\mathbf{U}_i^v$, $\mathbf{U}_i^h$, and $\mathbf{\Phi}_i^h$, calculate the optimal $\mathbf{\Phi}_{i+1}^v$ using (9).
5: Given $\mathbf{\Phi}_{i+1}^v$, calculate the optimal $\mathbf{\Phi}_{i+1}^h$ using (10).
6: Given $\mathbf{\Phi}_{i+1}^v$, $\mathbf{\Phi}_{i+1}^h$, and $\mathbf{U}_i^v$, calculate the optimal $\mathbf{U}_{i+1}^h$ using (11).
7: Given $\mathbf{U}_{i+1}^v$, $\mathbf{U}_{i+1}^h$, $\mathbf{\Phi}_{i+1}^v$, $\mathbf{\Phi}_{i+1}^h$, and η_{i+1}, calculate $\mathbf{w}_{i+1}$ and η_{i+2} using (7) and (8), respectively.
8: Update $i = i + 1$.
9: **until** the objective value of (P1) converges or the maximum number of iterations are completed.
10: Perform the QAM+RP modulation as described in subsections 4.3, 4.4, and 4.5.
11: Retrieve $\hat{\lambda}$ and $\hat{y}$ using (P2) and (14), respectively.
12: Use $\hat{\lambda}$ and $\hat{y}$ for QAM and RP demodulation, respectively, and calculate bit error.

5 Results and discussion

5.1 Numerical analysis

In this section, we provide the numerical analysis results of the proposed scheme to compare its performance with some closely related works. For the simulation setup, a MISO downlink system is considered, as shown in Fig. 3, where an IRS assists the AP to communicate with a user whose direct channel to the AP is weak. The AP and IRS are in fixed locations, and the Rician model is assumed for the AP-IRS link, whereas the AP-User and IRS-User links are modeled as Rayleigh fading channels. The AP-IRS distance, denoted by d_o, is fixed to 50 m, and the user has a 2-meter vertical distance (d_v) from the

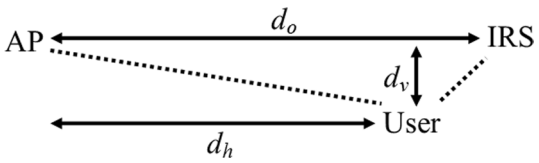

Fig. 3 Simulation setup

line connecting the AP and IRS. Furthermore, the horizontal distance between the AP and user, denoted by d_h, is varied to observe the change in performance. After setting d_h, d_o, and d_v, we can easily calculate the direct distances between the AP, IRS, and user, which are used to determine the path loss for each link as follows:

$$PL(\text{dB}) = C_o + 10a \log\left(\frac{d}{D_o}\right), \tag{15}$$

where C_o is the path loss (dB) at a reference distance of D_o and a is the path-loss exponent, whereas d is the distance of a link. We assume $a = 2.2$, 3.5, and 2.5 for the AP-IRS link, AP-User link (weak channel), and IRS-User link, respectively. The path loss at a reference distance of 1 m, C_o, is set to 30 dB and $d_h = 47$ m unless stated otherwise. The total transmit power P_t at the AP is assumed to be 40 dBm, whereas the noise power (σ^2) at the user is -96 dBm. Additionally, the amplitude of each reflecting element of the DP-IRS is normalized by a factor of $\frac{1}{\sqrt{2}}$, i.e., $\frac{1}{\sqrt{2}}\boldsymbol{\Psi}$.

In Fig. 4, we plot the convergence behavior of Algorithm 1 for different values of N_t and N. It can be observed that Algorithm 1 takes only 2 iterations to reach convergence for all values of N_t and N.

For $N_t = 2$ and 6 bits of data transmission per channel use, Fig. 5 shows the BER performance versus the number of reflecting elements. The compared schemes are enumerated below.

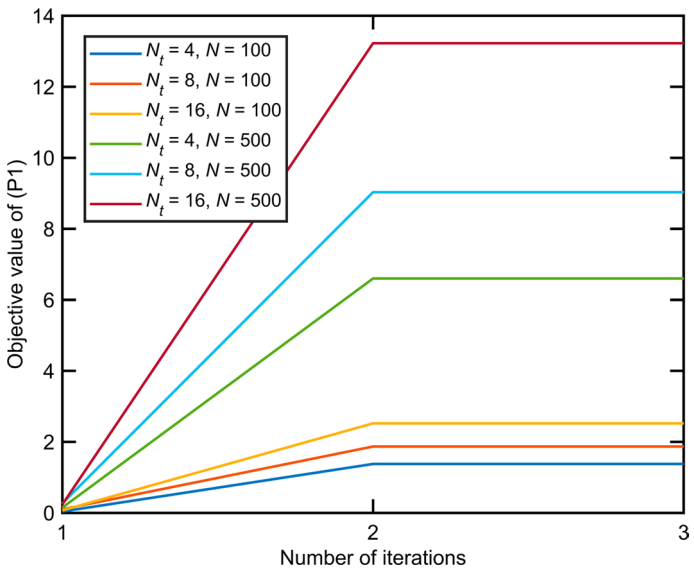

Fig. 4 Convergence behavior of Algorithm 1 for various values of N_t and N

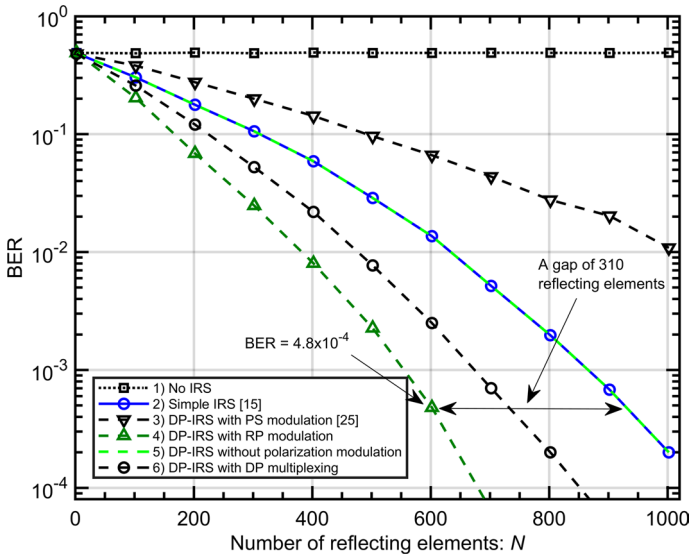

Fig. 5 BER versus the number of reflecting elements for $N_t = 2$

1) No IRS: There is no IRS in the network, and the precoder $\mathbf{w}$ is set to $\sqrt{p}\frac{\mathbf{h}_d}{\|\mathbf{h}_d\|}$. To transmit 6 bits per channel use, 64-QAM modulation is used. In Fig. 5, it is seen that without IRS, the user achieves the worst BER performance.
2) Simple IRS: In this scheme, a simple IRS employs AO [15] to maximize the SNR at the user. To transmit 6 bits per channel use, 64-QAM is assumed.
3) DP-IRS with PS modulation: A DP-IRS assists the communication by performing PS modulation [25]. To transmit 6 bits per channel use, 5 bits are modulated in a 32-QAM symbol, and the remaining bit is sent by switching between polarizations. Figure 5 shows that the BER performance is lower than that of the simple IRS and our proposed scheme. This is because when the PS modulation modulates 1 bit via polarization switching, it makes inefficient use of the DP-IRS. Specifically, only one polarization v/h is activated at a time, depending on the data bit 0/1.
4) DP-IRS with RP modulation: Here, we consider the DP-IRS with the proposed scheme, i.e., Algorithm 1. To transmit 6 bits per channel use, 4 bits are modulated in a 16-QAM symbol, while 2 bits are modulated based on the RP modulation. Although we send the same number of bits as the non-IRS and simple IRS schemes, a lower-order modulation (16-QAM) is utilized. In Fig. 5, it can be seen that the proposed scheme outperforms the other schemes by a large gap.
5) DP-IRS without polarization modulation: Here, we do not create a phase difference between the polarized signals. At the receiver, we add the signals coherently to generate a combined signal for demodulation. Figure 5 shows that the performance of this scheme is exactly the same as that of simple IRS. This result is obvious because the total power reflected by N elements of the simple IRS and DP-IRS is the same. Furthermore, both polarizations experience the same channel gains, and a single-RF-chain DP antenna radiates the same QAM symbol on both polarizations with equally divided power, which is directed toward a single user with no PM.

6) DP-IRS with DP multiplexing: In this scheme, we use the orthogonal property of DP to transmit and receive two independent data streams. At the receiver, we do not combine them coherently; instead, both data streams are processed and demodulated independently. To transmit 6 bits per channel use, we use two 8-QAM symbols, i.e., one for each polarization. Figure 5 shows that multiplexing two data streams achieves better performance as compared to many benchmark schemes. However, this scheme needs two RF chains per DP-antenna, which increases the hardware cost and is against our proposed system architecture.

Overall, in Fig. 5, except for the "No IRS" case, we observe that increasing N improves BER performance for all schemes. In Fig. 5, we also note that the DP-IRS requires 34% less reflecting elements as compared to the simple IRS to achieve BER $= 4.8 \times 10^{-4}$. In particular, as shown in Fig. 5, for BER $= 4.8 \times 10^{-4}$, DP-IRS and simple IRS require 600 and 910 reflecting elements, respectively.

In the following simulation results, we include another scheme proposed in [27], where a DP-IRS is used to modulate data directly on the reflecting elements. In this scheme, the DP-IRS is connected to an information source device, whereas a simple RF source, which has no amplitude- and phase-changing capabilities, throws RF signals onto the reflecting elements. The amplitudes and phases of the reflected waves are controlled such that they are coherently added at the user to create a modulation symbol. A summary of all compared schemes is given in Table 1.

For $N_t = 1$ and 5 bits per channel use, we include the scheme in [27] for comparison in Fig. 6. The reason for selecting $N_t = 1$ is that the scheme in [27] assumes a simple RF source, which is not capable of precoding. If the practical limitations mentioned in [27] are neglected, an ideal QAM modulation results in nearly the same BER performance as the simple IRS, as shown in Fig. 6. The small performance difference is due

Table 1 Summary of the compared schemes

Scheme	Configuration	Modulation	Observation
No IRS	There is no IRS in the network and only AP-user link exists	QAM	Poor performance because of no IRS link
Simple IRS	The network is assisted by the single-polarized IRS	QAM	Good performance
DP-IRS with PS modulation	The network is assisted by the DP-IRS and PS modulation is used	QAM and PS modulation	Poor performance because of the inefficient use of DP-IRS
DP-IRS with RP modulation	The network is assisted by the DP-IRS with the proposed scheme	QAM and RP modulation	Best performance
DP-IRS without polarization modulation	The network is assisted by the DP-IRS without any polarization modulation	QAM	Same performance as a simple IRS
DP-IRS with DP multiplexing	The network is assisted by the DP-IRS to multiplex two data streams	QAM	Good performance because of two independent data streams
Modulation on the DP-IRS' elements [27]	The data are modulated directly on the reflecting elements for DP multiplexing	QAM	Poor performance because of no AP-user link

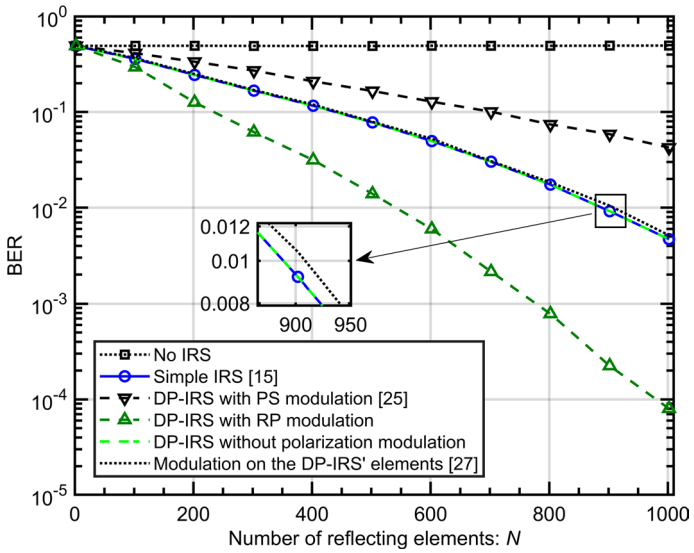

Fig. 6 BER versus the number of reflecting elements for $N_t = 1$

to the absence of the AP-User direct link. This modulation scheme does not require complex RF chains at the AP, as the modulation task is transferred to the DP-IRS. In Fig. 7, we compare the different combinations of K-QAM and L-RP modulation levels in terms of BER performance for $N_t = 4$ and $C_o = 25$. We consider a simple IRS transmitting 10 bits per channel use with 1024-QAM modulation and DP-IRS transmitting 10 bits per channel use with the combination of 256-QAM and 4-RP. Figure 6 shows that this DP-IRS scheme achieves significantly better BER performance than the simple IRS while providing the same SE. In Fig. 7, we also compare the DP-IRS with 11, 12, and 13 bits per channel use with the combinations of (512-QAM + 4-RP), (1024 -QAM + 4-RP), and (2048-QAM + 4-RP), respectively. These combinations exhibit

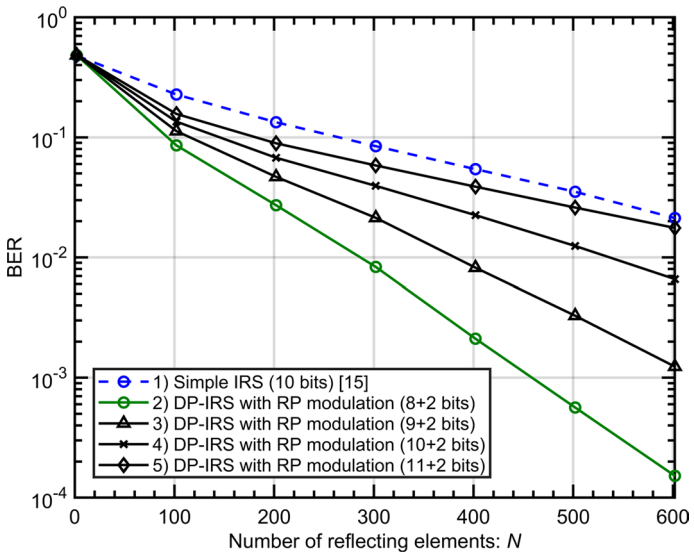

Fig. 7 Combination of different levels of the QAM and RP modulations

the improved BER and SE performance compared to the simple IRS; however, they have worse BER performances than the DP-IRS with $(8 + 2)$-bit combination at the cost of higher SE.

In Figs. 8 and 9, we vary d_h and N_t, respectively, and plot the BER performance for $N = 200$ and $N = 500$, respectively. For these simulations, we transmit 10 bits per channel use. We observe that as the user moves closer to the IRS, the BER performance improves. Similarly, as the number of transmit antennas increases, the proposed scheme outperforms the other schemes by a larger gap.

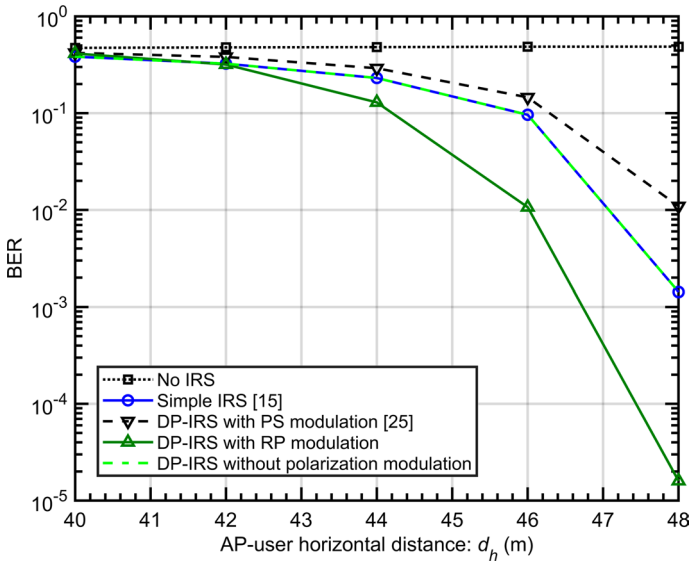

Fig. 8 BER versus AP-user horizontal distance for $N_t = 4$ and $N = 500$

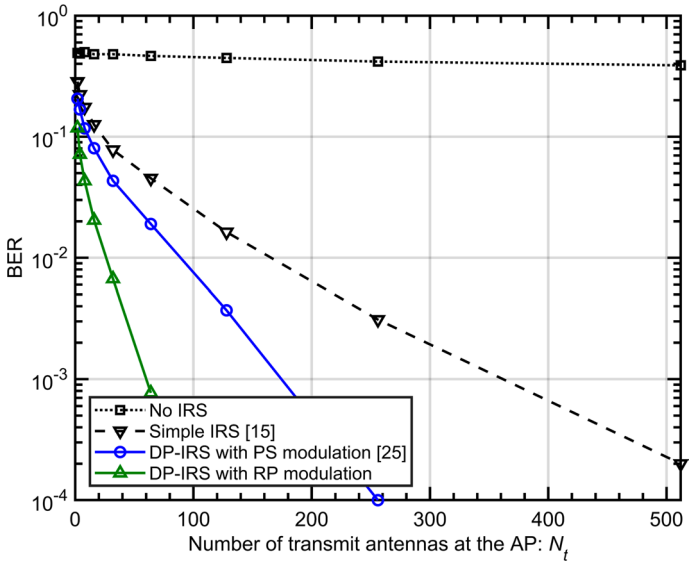

Fig. 9 BER versus the number of transmit antennas for $N = 200$

5.2 Extension to the system with multiple receive antennas

In the ensuing discussion, we explore the expansion of this study to encompass MIMO scenarios featuring multiple receive antennas. The consideration of multiple receive antennas within the framework of our proposed scheme introduces a distinct optimization challenge. This complexity arises due to the intricate nature of the optimization problem, primarily attributed to the fact that any phase shift introduced in a single reflecting element results in a uniform phase shift across all receive antennas. Consequently, the task of maximizing the SE performance of such a system, while simultaneously preserving a specific phase difference at each receive antenna, poses a formidable challenge.

To elaborate further, the DP-IRS-assisted MIMO network is illustrated in Fig. 10. In this configuration, the AP and user are endowed with N_t and N_r DP antennas, respectively. The signal model presented in (2) can be extended to encompass N_t transmit antennas, N receive antennas, and N reflecting elements:

$$\begin{aligned}\mathbf{y} = \mathbf{W}\Big[&\mathbf{E}_v\{\mathbf{H}_{r,vv}^H\boldsymbol{\Phi}_{vv}\mathbf{G}_v + \mathbf{H}_{r,hv}^H\boldsymbol{\Phi}_{hv}\mathbf{G}_h + \mathbf{H}_{d,v}^H\}\mathbf{U}_v \\ &+\mathbf{E}_h\{\mathbf{H}_{r,hh}^H\boldsymbol{\Phi}_{hh}\mathbf{G}_h + \mathbf{H}_{r,vh}^H\boldsymbol{\Phi}_{vh}\mathbf{G}_v + \mathbf{H}_{d,h}^H\}\mathbf{U}_h\Big]\mathbf{F}\mathbf{s} + \mathbf{W}\mathbf{z},\end{aligned} \tag{16}$$

where $\mathbf{z}$, $\mathbf{s}$, $\mathbf{F} \in {}^{N_t\times N_s}$, $\mathbf{W} \in {}^{N_r\times N_s}$, $\mathbf{E}_p \in {}^{N_r\times N_r}$, $\mathbf{U}_p \in {}^{N_t\times N_t}$, $\mathbf{G} \in {}^{N\times N_t}$, $\mathbf{H}_r^H \in {}^{N_r\times N}$, and $\mathbf{H}_d^H \in {}^{N_r\times N_t}$ denote circularly symmetric complex Gaussian noise vector at the user, transmitted symbol vector at the AP, transmit digital filter, receive digital filter, receive vertical/horizontal phase shifts, transmit vertical/horizontal phase shifts, AP-IRS channel, IRS-user channel, and AP-user channel, respectively, where $p \in \{v, h\}$. For further elaboration on the system model of the DP-IRS-assisted MIMO network, additional details can be found in [31]; however, these details are omitted in this context for conciseness.

Let $\mathbf{H} = \mathbf{E}_v\{\mathbf{H}_{r,vv}^H\boldsymbol{\Phi}_{vv}\mathbf{G}_v + \mathbf{H}_{r,hv}^H\boldsymbol{\Phi}_{hv}\mathbf{G}_h + \mathbf{H}_{d,v}^H\}\mathbf{U}_v + \mathbf{E}_h\{\mathbf{H}_{r,hh}^H\boldsymbol{\Phi}_{hh}\mathbf{G}_h + \mathbf{H}_{r,vh}^H\boldsymbol{\Phi}_{vh}\mathbf{G}_v + \mathbf{H}_{d,h}^H\}\mathbf{U}_h$ denote the composite MIMO channel. The spectral efficiency of the system is then given by $\log_2 \det(\mathbf{I} + \mathbf{W}^\dagger\mathbf{H}\mathbf{F}\mathbf{F}^H\mathbf{H}^H\mathbf{W})$. The problem formulation, within the context of our proposed scheme, can now be expressed as follows:

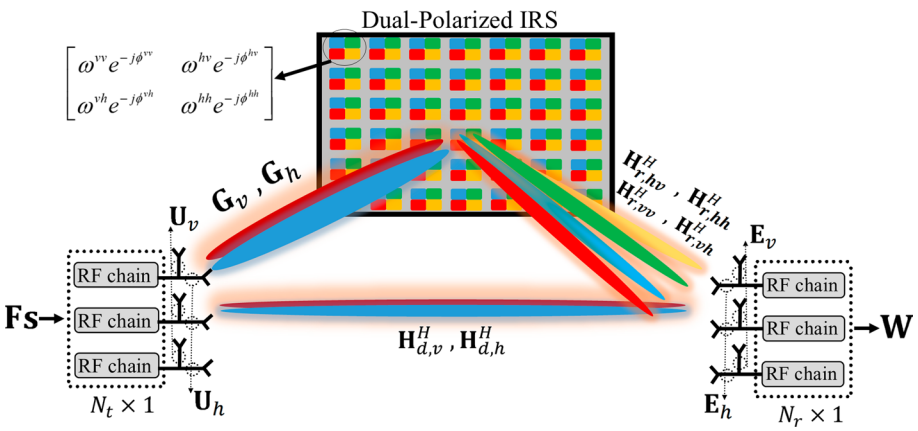

Fig. 10 DP-IRS-assisted MIMO network

$$
\begin{aligned}
&\max_{\mathbf{W},\mathbf{F},\mathbf{U}_p,\mathbf{E}_p,\Phi_{pq}} \log_2 \det(\mathbf{I} + \mathbf{W}^{\dagger}\mathbf{H}\mathbf{F}\mathbf{F}^H\mathbf{H}^H\mathbf{W}) \\
&\text{s.t.} \quad \mathbf{H} = \mathbf{E}_v\left\{\mathbf{H}_{r,vv}^H\Phi_{vv}\mathbf{G}_v + \mathbf{H}_{r,hv}^H\Phi_{hv}\mathbf{G}_h + \mathbf{H}_{d,v}^H\right\}\mathbf{U}_v \\
&\quad + \mathbf{E}_h\left\{\mathbf{H}_{r,hh}^H\Phi_{hh}\mathbf{G}_h + \mathbf{H}_{r,vh}^H\Phi_{vh}\mathbf{G}_v + \mathbf{H}_{d,h}^H\right\}\mathbf{U}_h, \\
&\quad \Phi_{pq} = \text{diag}(e^{-j\phi_{pq,1}}, e^{-j\phi_{pq,2}}, e^{-j\phi_{pq,3}}, \ldots, e^{-j\phi_{pq,N}}), p, q \in \{v, h\}, \\
&\quad \mathbf{E}_p = \text{diag}(e^{-j\gamma_{p,1}}, e^{-j\gamma_{p,2}}, e^{-j\gamma_{p,3}}, \ldots, e^{-j\gamma_{p,N_r}}), p \in \{v, h\}, \\
&\quad \mathbf{U}_p = \text{diag}(e^{-j\zeta_{p,1}}, e^{-j\zeta_{p,2}}, e^{-j\zeta_{p,3}}, \ldots, e^{-j\zeta_{p,N_r}}), p \in \{v, h\}, \\
&\quad \arg\left(y_{n_r}^v\right) = 0, n_r = 1, 2 \ldots, N_r, \\
&\quad \arg\left(y_{n_r}^h\right) = \lambda_{n_r}, n_r = 1, 2 \ldots, N_r, \\
&\quad \|\mathbf{F}\|^2 \leq P_t.
\end{aligned}
\tag{P2}
$$

The objective function of (P2) exhibits non-concavity over $\mathbf{\Phi}_{pq}$, $\mathbf{U}_p$, and $\mathbf{E}_p$. The unimodular restrictions within the second and third constraints of (P2) also demonstrate non-convexity. Additionally, the signal received at polarization p of DP antenna n_r, denoted as $y_{n_r}^p$, undergoes a phase shift from all reflecting elements. Consequently, the formulation of a specific phase difference λ_{n_r} at the n_rth DP antenna poses a challenging problem. However, the resolution of (P2) optimally remains a non-trivial challenge, and while there is currently no standard method, the investigation of potential solutions to this problem will be a focal point in our future research.

It is worth mentioning that, to focus on the gains of the proposed scheme in the considered MISO system where there is no polarization diversity, polarization multiplexing, or interference, the optimal Φ_{pq} was simply set equal to Φ_{pp}. However, in the presence of polarization diversity in MISO systems or in MIMO configurations, the anti-diagonal entries of (1) cannot be equated to diagonal entries and therefore require appropriate solutions. Nonetheless, in MISO systems, the solution to the anti-diagonal entries of (1) can be straightforwardly derived as closed-form solutions similar to the diagonal entries of (1), as detailed in Section 4.2. However, in MIMO configurations, i.e., (P2), more complex solutions or convex relaxations might be necessary to obtain feasible solutions.

5.3 Discussion

5.3.1 Practical constraints

We discuss the possible practical constraints that an IRS hardware setup can introduce in problems (P1) and (P2), and their potential impact on performance. Specifically, some of the main practical constraints are as follows:

1. Reflection Amplitude as a Function of Phase Shift: In practical IRS designs, such as metamaterials, the amplitude of the reflecting signal becomes a function of the phase shift induced in the element, denoted as $\alpha = f(\theta)$, where α represents the reflection amplitude and θ denotes the phase shift. Further details on this issue are provided in [2]. However, if the size of each element is smaller than the wavelength, then each meta-element provides very uniform scattering, resulting in consistent amplitudes for all phase shift values. Hence, given the element size is sub-wavelength at the working frequency, this practical constraint can be ignored in the problem. How-

ever, if the element size is not sub-wavelength, it is necessary to take into account the reflecting amplitudes while optimizing the phase shifts in problems (P1) and (P2).

2. Discrete Phases Instead of Continuous: In practical metasurface setups, we encounter discrete values of phase shifts to select instead of continuous phase shift values. One straightforward approach to deal with this is to solve the problem for continuous phase shifts and then select the nearest available discrete values. In [2], it has been shown that having at least 3 bits of control, i.e., at least 8 discrete phase shift values, yields near-continuous phase shift performance in MISO systems. However, the impact of discrete values is more prominent in MIMO configurations, where discrete phases can result in lower performance compared to continuous phases due to multiuser interference. Therefore, achieving high-resolution control may be required to attain near-continuous phase performance.
3. Non-Ideal Polarization: In practical IRS setups, similar to conventional DP antennas, it is possible that inverse cross-polarization degrades the orthogonality nature of DP waves. In such scenarios, it is important to take into account the values of inverse cross-polarization factors while solving problems (P1) and (P2).

Although these constraints can be readily accounted for solving P1 and P2, their impact can provide interesting insights into the performance of the proposed scheme. Especially owing to the aforementioned reasons, the impact is expected to be more pronounced in multiuser or multistream scenarios, i.e., (P2). Nevertheless, the inclusion of these practical impairments or constraints is an interesting research direction for the readers and will be considered in our future works.

5.3.2 Performance upper bounds

We now discuss the upper bound on the performance of the proposed algorithm by examining the optimality of solutions for each subproblem.

1. For the transmit active beamforming, denoted as $\mathbf{w}$, we propose a maximum ratio transmission-based solution (7), which is a well-known optimal solution for MISO wireless networks
2. We now analyze the optimization problem concerning the DP-IRS phases. The objective value of (P1.3) can be upper bounded as follows:

$$\left|\left(\mathbf{l}^{\nu}\right)^{H}\boldsymbol{\alpha}^{\nu}+\beta^{'\nu}\right| \leq \left|\left(\mathbf{l}^{\nu}\right)^{H}\boldsymbol{\alpha}^{\nu}\right|+\left|\beta^{'\nu}\right|. \tag{17}$$

To achieve this upper bound, we should have $\arg\left(\left(\mathbf{l}^{\nu}\right)^{H}\boldsymbol{\alpha}^{\nu}\right)=\arg\left(\beta^{'\nu}\right)$. Hence, the solution proposed in (9), which satisfies $\arg\left(\left(\mathbf{l}^{\nu}\right)^{H}\boldsymbol{\alpha}^{\nu}\right)=\arg\left(\beta^{'\nu}\right)$, is optimal. The problems (P1.5) and (P1.7) share a similar mathematical structure to (9). Consequently, the closed-form solutions derived for these problems are also optimal and represent upper bounds.

3. For selecting the receiver phase shifters, we employ the maximum likelihood method. This approach is again known to be optimal and serves as an upper bound on achievable performance.

We understand that the AO algorithm results in a performance gap due to the iterations. However, given the optimal solutions, it is observable from Fig. 4 that the proposed algorithm achieves a convergence value with only a single iteration. Although the algorithm runs for two iterations to satisfy the termination criteria, the performance value does not change after a single iteration. Thus, there is no performance loss due to multiple iterations. However, at this point, we are uncertain whether the algorithm converges to the global optimal solution or a local one. We believe that further research work on the analytical analysis of the proposed scheme could potentially provide insights into the upper bounds.

6 Conclusion

In this paper, we propose a scheme that exploits the orthogonal property of a DP-IRS to improve the BER and SE performance of the network compared to that of the simple IRS. In the proposed scheme, we control the AP precoder and DP-IRS phases to maximize the signal power and generate a specific phase difference between the vertical and horizontal polarized signals. We recover the phase difference at the user and use it to align the polarized signals, which are then combined coherently. The recovered phase difference and the transmitted signal both contain bits of information. To optimize the proposed scheme, we formulate an SNR maximization problem, which is further divided into three subproblems. The first two subproblems, which are related to the vertical and horizontal polarized signals, are solved in an alternating manner, whereas for the third subproblem, the maximum likelihood algorithm is applied to estimate the phase shift. Finally, we evaluate the performance of the proposed scheme based on numerical analysis and compare it with other closely related works. The simulation results show that the proposed scheme significantly improves the network's SE and BER performance compared to the conventional schemes. Furthermore, the performance gap widens as we increase the number of reflecting elements. We note that SNR maximization and data modulation are typically two of the primary operations of a general wireless network's physical layer; thus, the proposed scheme is applicable to DP-IRS-assisted systems for future wireless networks. An interesting future work could be investigating the extension of this work to multiuser scenarios with more practical considerations, such as hardware-constrained reflection at DP-IRS, polarization power leakage, discrete phases, and imperfect/partial channel state information. An analytical analysis of the proposed system could potentially offer insights into the upper bounds and represents another interesting and intriguing future research direction.

Abbreviations

SNR	Signal-to-noise ratio
DP	Dual polarization
SE	Spectral efficiency
BER	Bit-error-rate
IRS	Intelligent reflecting surface
RIS	Reconfigurable intelligent surface
AO	Alternating optimization
MISO	Multiple-input single-output
MIMO	Multiple-input multiple-output
PD	Polarization diversity
PM	Polarization MULTIPLEXING
PS-QPSK	Polarization-switched quadrature phase shift keying
DP-IRS	Dual-polarized intelligent reflecting surface

RF	Radio-frequency
AP	Access point
RP	Relative phase
QAM	Quadrature amplitude modulation

Author contributions
MM and KL both contributed to the formulation of the research problem, development of algorithms, numerical simulations, and writing of the paper. Both authors read and approved the manuscript.

Funding
This work was supported in part by the Basic Science Research Program through the National Research Foundation of Korea (NRF) funded by the Ministry of Education under Grant NRF-2019R1A6A1A03032119 and in part by the NRF Grant funded by the Korean Government (MSIT) under Grant NRF-2022R1A2C1006566.

Availability of data and materials
The datasets used and/or analyzed during the current study are available from the corresponding author upon reasonable request.

Declaration

Ethics approval and consent to participate
N/A

Consent for publication
N/A

Competing interest
The authors declare that they have no competing interest.

Received: 11 December 2023 Accepted: 12 April 2024
Published online: 08 May 2024

References

1. D.M. Pozar, S.D. Targonski, H. Syrigos, Design of millimeter wave microstrip reflectarrays. IEEE Trans. Antennas Propag. **45**, 287–296 (1997)
2. S. Abeywickrama, R. Zhang, Q. Wu, C. Yuen, Intelligent reflecting surface: practical phase shift model and beamforming optimization. IEEE Trans. Commun. **68**, 5849–5863 (2020)
3. T.J. Cui, M.Q. Qi, X. Wan, J. Zhao, Q. Cheng, Coding metamaterials, digital metamaterials and programmable metamaterials. Light Sci. Appl. **3**, e218 (2014)
4. J. Zhao, A survey of intelligent reflecting surfaces (IRSs): Towards 6G wireless communication networks. arXiv preprint arXiv:1907.04789 (2019)
5. E. Basar, M. Di Renzo, J. De Rosny, M. Debbah, M.-S. Alouini, R. Zhang, Wireless communications through reconfigurable intelligent surfaces. IEEE Access **7**, 116753–116773 (2019)
6. C. Huang, A. Zappone, G.C. Alexandropoulos, M. Debbah, C. Yuen, Reconfigurable intelligent surfaces for energy efficiency in wireless communication. IEEE Trans. Wirel. Commun. **18**, 4157–4170 (2019)
7. M.A. ElMossallamy, H. Zhang, L. Song, K.G. Seddik, Z. Han, G.Y. Li, Reconfigurable intelligent surfaces for wireless communications: principles, challenges, and opportunities. IEEE Trans. Cogn. Commun. Netw. **6**, 990–1002 (2020)
8. X. Tan, Z. Sun, D. Koutsonikolas, J. M. Jornet, Enabling indoor mobile millimeter-wave networks based on smart reflect-arrays, in *Proc. IEEE Infocom Conf. Comput. Commun.* pp. 270–278 (2018)
9. X. Tan, Z. Sun, J. M. Jornet, D. Pados, Increasing indoor spectrum sharing capacity using smart reflect-array, in *Proc. IEEE Int. Conf. Commun. (ICC)*, pp. 1–6 (2016)
10. S. Nie, J. M. Jornet, I. F. Akyildiz, Intelligent environments based on ultra-massive MIMO platforms for wireless communication in millimeter wave and terahertz bands, in *Proc. IEEE Int. Conf. Acoust., Speech and Signal Process. (ICASSP)*, pp. 7849-7853 (2019)
11. E. Basar, Reconfigurable intelligent surface-based index modulation: A new beyond MIMO paradigm for 6G. IEEE Trans. Commun. **68**, 3187–3196 (2020)
12. C. Liaskos, A. Tsioliaridou, S. Nie, A. Pitsillides, S. Ioannidis, I. Akyildiz, An interpretable neural network for configuring programmable wireless environments, in *Proc. IEEE 20th Int. Workshop Signal Process. Advances in Wireless Commun. (SPAWC)*, pp. 1–5 (2019)
13. D. Mishra, H. Johansson, Channel estimation and low-complexity beamforming design for passive intelligent surface assisted MISO wireless energy transfer, in *Proc. IEEE Int. Conf. Acoust., Speech and Signal Process. ICASSP)*, pp. 4659–4663 (2019)
14. C. Huang, A. Zappone, M. Debbah, C. Yuen, Achievable rate maximization by passive intelligent mirrors, in *Proc. IEEE Int. Conf. Acoust., Speech and Signal Process. (ICASSP)*, pp. 3714–3718 (2018)
15. Q. Wu, R. Zhang, Intelligent reflecting surface enhanced wireless network via joint active and passive beamforming. IEEE Trans. Wirel. Commun. **18**, 5394–5409 (2019)
16. M. Munawar, K. Lee, Low-complexity adaptive selection beamforming for IRS-assisted single-user wireless networks. IEEE Trans. Veh. Technol. 1-6 (2022)

17. Q. Wu, R. Zhang, Beamforming optimization for wireless network aided by intelligent reflecting surface with discrete phase shifts. IEEE Trans. Commun. **68**, 1838–1851 (2019)
18. X. Yu, D. Xu, R. Schober, MISO wireless communication systems via intelligent reflecting surfaces, in *Proc. IEEE Int. Conf. Commun. China (ICCC)*, pp. 735–740 (2019)
19. B. Ning, Z. Chen, W. Chen, J. Fang, Beamforming optimization for intelligent reflecting surface assisted MIMO: a sum-path-gain maximization approach. IEEE Wirel. Commun. Lett. **9**, 1105–1109 (2020)
20. X. Yu, D. Xu, R. Schober, Optimal beamforming for MISO communications via intelligent reflecting surfaces, in *Proc. IEEE 21st Int. Workshop Signal Process. Advances Wireless Commun. (SPAWC)*, pp. 1–5 (2020)
21. X. Ma, Z. Chen, W. Chen, Z. Li, Y. Chi, C. Han, S. Li, Joint channel estimation and data rate maximization for intelligent reflecting surface assisted terahertz MIMO communication systems. IEEE Access **8**, 99565–99581 (2020)
22. Z. Wang, L. Liu, S. Cui, Channel estimation for intelligent reflecting surface assisted multiuser communications: framework, algorithms, and analysis. IEEE Trans. Wirel. Commun. **19**, 6607–6620 (2020)
23. R.G. Vaughan, Polarization diversity in mobile communications. IEEE Trans. Veh. Technol. **39**, 177–186 (1990)
24. L. Deng, J. Deng, Z. Guan, J. Tao, Y. Chen, Y. Yang, D. Zhang, J. Tang, Z. Li, Z. Li et al., Malus-metasurface-assisted polarization multiplexing. Light Sci. Appl. **9**, 1–9 (2020)
25. B. Krongold, T. Pfau, N. Kaneda, S.C.J. Lee, Comparison between PS-QPSK and PDM-QPSK with equal rate and bandwidth. IEEE Photon. Technol. Lett. **24**, 203–205 (2011)
26. A. S. De Sena, P. H. Nardelli, D. B. Da Costa, F. R. M. Lima, L. Yang, P. Popovski, Z. Ding, C.B. Papadias, IRS-assisted massive MIMO-NOMA networks: exploiting wave polarization. IEEE Trans. Wireless Commun. (2021)
27. X. Chen, J.C. Ke, W. Tang, M.Z. Chen, J.Y. Dai, E. Basar, S. Jin, Q. Cheng, T.J. Cui, Design and implementation of MIMO transmission based on dual-polarized reconfigurable intelligent surface. IEEE Wirel. Commun. Lett. **10**, 2155–2159 (2021)
28. B. Clerckx, C. Oestges, Chapter 3 - Analytical MIMO Channel Representations for System Design, in *Mimo Wireless Networks*, 2nd edn., ed. by B. Clerckx, C. Oestges (Academic Press, Oxford, 2013), pp.78–80
29. H. Arai, K. Abe, N. Takemura, T. Mitsui, Dual-polarized switched beam antenna with variable phase shifter, in *Proc. Int. Workshop on Antenna Technol. (IWAT)*, pp. 19–22 (2013)
30. J. Shu, H.-L. Peng, Y.-P. Zhang, J.-F. Mao, A dual polarized pattern reconfigurable antenna array using liquid crystal phase shifter, in *Proc. Int. Symp. on Antennas and Propag. (ISAP)*, pp. 1–2 (2018)
31. M. Munawar, K. Lee, Dual-polarized IRS-assisted MIMO network. IEEE Trans. Wirel. Commun. 1–1 (2023)
32. S. Sun, W. Jiang, S. Gong, T. Hong, Reconfigurable linear-to- linear polarization conversion metasurface based on PIN diodes. IEEE Antennas Wirel. Propag. Lett. **17**(9), 1722–1726 (2018)
33. J. Wang, R. Yang, R. Ma, J. Tian, W. Zhang, Reconfigurable multifunctional metasurface for broadband polarization conversion and perfect absorption. IEEE Access **8**, 105815–105823 (2020)
34. H.F. Ma, G.Z. Wang, G.S. Kong, T.J. Cui, Independent controls of differently-polarized reflected waves by anisotropic metasurfaces. Sci. Rep. **5**(1), 9605 (2015)

Publisher's Note